Journal of Oceanography, Vol. 61, pp. 479 to 492, 2005

Structure and Transport of the Agulhas Current and Its Temporal Variability

HARRY L. BRYDEN[1]*, LISA M. BEAL[2] and LOUISE M. DUNCAN[1]

[1]*Southampton Oceanography Centre, Southampton SO14 3ZH, U.K.*
[2]*Rosenstiel School of Marine and Atmospheric Science, University of Miami, FL 33149, U.S.A.*

(Received 21 November 2003; in revised form 1 November 2004; accepted 8 November 2004)

Using a year-long moored array of current meters and well-sampled synoptic sections, we define the variability and mean structure and transport of the Agulhas current. Nineteen current meter records indicate that time scales for the temporal variability in the alongshore and offshore velocities are 10.2 and 5.4 days, respectively. Good vertical correlation exists between the alongshore or onshore velocity fluctuations, excluding the Agulhas Undercurrent. The lateral scale for the thermocline Agulhas current is about 60 km and the onshore velocity correlations are positive throughout the Agulhas Current system. Mean velocities from the array determine that the offshore edge of the Agulhas Current lies at 203 km and the penetration depth is 2200 m offshore of the Undercurrent. Hence, daily averaged velocity sections, determined by interpolation and extrapolation of current meter locations, for a 267-day period, from the surface to 2400 m depth and from the coast out to 203 km offshore encompass the main features of the Agulhas Current system. The Agulhas current is generally found close to the continental slope, within 31 km of the coast for 211 of 267 days. There are only five days when the core of the current is found offshore at 150 km. Total transport is always poleward, varying from –121 to –9 Sv, with maximum transport occurring when the core is 62 km from the coast. Average total transport for the 267 day period is –69.7 Sv; the standard deviation in daily transport values is 21.5 Sv; and the mean transport has an estimated standard error of 4.3 Sv. The Agulhas Undercurrent, which hugs the continental slope below the zero velocity isotach, has an average equatorward transport of 4.2 Sv, standard deviation of 2.9 Sv and an estimated standard error of 0.4 Sv. Transports from the moored array are in reasonable agreement with transport results from synoptic sections. Based on time series measurements at about 30° latitude in each ocean basin, the Agulhas Current is the largest western boundary current in the world ocean.

Keywords:
· Agulhas Current,
· Agulhas Undercurrent,
· western boundary currents,
· Sverdrup transport,
· circulation,
· boundary current variability.

1. Introduction

Western boundary currents are the most striking manifestation of basin-scale ocean circulation, yet it is surprising how little we know about their sizes. It is generally considered that the Gulf Stream in the North Atlantic Ocean is the largest of the western boundary currents; there is some uncertainty whether the Agulhas Current in the Indian Ocean or the Kuroshio in the North Pacific is second largest; and the Brazil Current in the South Atlantic and East Australian Current in the South Pacific are thought to be considerably smaller. As part of the World Ocean Circulation Experiment (WOCE) plans to measure the transport and variability of western boundary currents at about 30°S in each ocean, we deployed a moored current meter array in the Agulhas Current southeast of Durban from February 1995 to April 1996.

Previous estimates for the transport of the Agulhas Current in this region have varied from 9 to 90 Sv (Beal, 1997). Much of the variation is due to differing assumptions used for geostrophic velocity profiles on single synoptic sections across the Agulhas Current and it is not clear whether the variation is due primarily to different structures in the synoptic sections or to different reference level choices. Two studies used measured currents to define the geostrophic reference levels. Grïndlingh (1980) matched geostrophic profiles on 8 synoptic sec-

* Corresponding author. E-mail: hlb@soc.soton.ac.uk

tions southeast of Durban to simultaneous current measurements made by lowering a current meter from the drifting ship to estimate an average transport above 1000 m depth of 62 Sv with little variation observed on the Port Edward section. Toole and Raymer (1985) averaged 1366 shipboard current, temperature and salinity profiles obtained by South African scientists with three additional historical hydrographic stations into 9 composite stations across the Agulhas Current to estimate an average Agulhas Current transport of 44 Sv.

To measure the strength of the Agulhas Current, we deployed 6 moorings on a section perpendicular to the South African coastline out from Port Edward (Fig. 1). Grïndlingh (1983) had shown that the variability in the position of the Agulhas Current was a minimum on this Port Edward section so a current meter array should most efficiently measure the structure and transport of the Agulhas Current and its variability here. During the mooring deployment cruise we made a combined CTD/LADCP section along the Port Edward section from which we identified a new current, the Agulhas Undercurrent, flowing equatorward along the continental slope below 800 m depth (Beal and Bryden, 1997) and we estimated the total synoptic transport of the Agulhas Current system to be 72 Sv by combining geostrophic and direct LADCP velocity profiles (Beal and Bryden, 1999). While such synoptic sections offer detailed information on the instantaneous structure and transport of the Agulhas Current, time series measurements are required to establish the extent to which the transport and structure of a synoptic section are representative of the time-averaged conditions for the western boundary current; for it is the time-averaged western boundary current transport that is needed to determine the basin-scale circulation and the heat and freshwater budgets for the Indian Ocean (Bryden and Beal, 2001). Thus, the moored array across the Agulhas Current is intended primarily to define the variability of the Agulhas Current system and then, in combination with a well-sampled synoptic section, to define the mean structure and transport of the western boundary current.

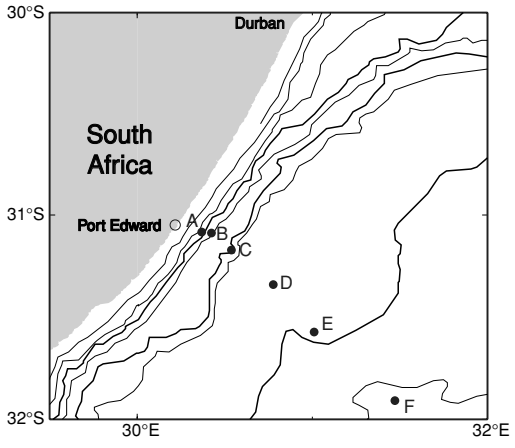

Fig. 1. Mooring deployment positions on the Port Edward section southeast of South Africa.

2. Description of the Measurements

The array deployed from *RRS Discovery* in February–March 1995 consisted of 6 moorings at distances of 13.4, 18.8, 32.4, 61.7, 101.9 and 152.8 km (A, B, C, D, E, F respectively) from the coast (Bryden *et al*., 1995). The array was recovered in April 1996 aboard *R/V Algoa*. The shallowest mooring (A) had been trawled up by a fishing boat in June 1995 and then dropped in shallower water, resulting in the loss of all instruments and data. After 13 months, mooring B parted below the intermediate buoyancy sphere; the upper portion with 2 instruments was recovered east of Cape Town on an emergency cruise

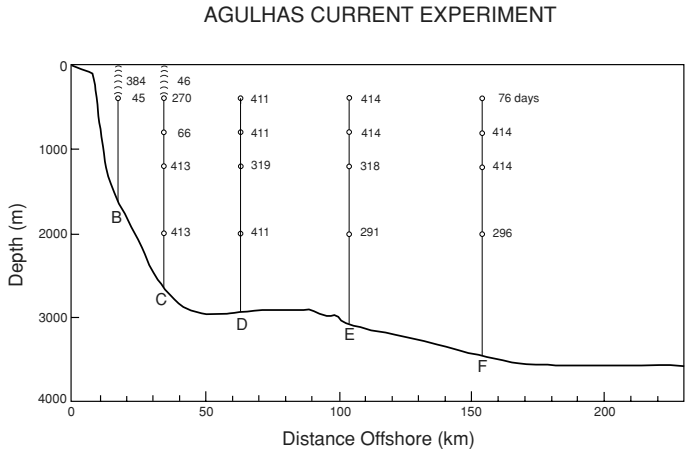

Fig. 2. Schematic of the recovered mooring array with the number of days of measurements recorded on each instrument.

aboard R/V *Algoa*; the lower portion, lying on the seabed, was not recovered during a dragging operation. The resulting data set consists of 16 Aanderaa current meter records with speed, direction, temperature and pressure at 30-minute intervals at nominal depths of 400, 800, 1200 and 2000 m depths on moorings C, D, E, F; two upward looking acoustic Doppler current profiler records on moorings B and C with east and north currents in 8 m bins from 400 m nominal depth up to about 50 m depth; and one FSI current meter record with speed, direction, temperature, pressure and salinity at 400 m nominal depth on mooring B. As is typical of moored arrays, the instrumental records are of varying length: 10 of the 19 instruments returned full-length records of about 400 days, while 4 instruments returned records shorter than 80 days. Notably, 15 instruments yielded records longer than 270 days (Fig. 2).

Each record is put through a Gaussian low-pass filter with half-width of 24 hours and subsampled to daily values. To match the orientation of the continental slope bathymetry, velocities are rotated into alongshore (40°T) and offshore (130°T) components. Using the daily pressure and temperature time series, temperatures at 400 and 800 m nominal depths are crudely corrected to a depth of 400 or 800 m at each mooring by using the vertical temperature gradient from nearby CTD stations taken during the deployment cruise.

Record-length mean and standard deviation for alongshore velocity and offshore velocity for each instrument are given in Table 1. The alongshore velocity is generally negative in the thermocline, indicating the poleward flowing Agulhas Current. Long time-averaged currents at the core of the Current above 100 m depth on mooring B are greater than 100 cm s^{-1}. Typical of western boundary currents with a poleward flowing warm core, the maximum poleward velocity moves offshore with depth; here the maximum average velocity at 400 m depth is on mooring B while the maximum at 800 m depth appears at

Table 1. Velocity time series in the Agulhas Current.

Instrument	Days	vd		uc		Pressure	
		Mean	Std	Mean	Std	Mean	Std
B100	382	–104.63	60.55	–1.55	9.82		
B200	382	–86.92	56.19	–0.41	8.83		
B300	382	–73.33	49.77	–0.87	7.31		
B400	382	–61.29	44.15	–1.38	6.17		
B440	43	–52.41	35.65	–19.62	16.13	430.09	4.53
C100	44	–85.29	42.22	0.40	12.68		
C200	44	–77.02	40.95	–0.78	11.47		
C300	44	–68.34	35.93	–0.19	10.22	364.92	8.48
C358	268	–56.84	29.29	3.05	9.67	387.38	18.10
C789	64	–27.63	14.46	1.10	7.24	810.49	9.84
C1156	411	0.65	14.15	–0.74	6.26	1189.29	14.93
C1967	411	9.48	9.10	1.53	3.43	2004.24	5.01
D375	409	–51.28	20.27	–0.35	18.23	448.75	46.83
D855	409	–35.21	16.67	–0.14	11.56	928.31	44.30
D1191	319	–19.58	13.04	–0.13	9.26	1257.86	36.75
D1955	409	–5.18	8.73	–1.93	6.79	2005.78	8.86
E401	411	–36.63	15.40	–7.70	15.27	437.00	35.33
E804	411	–25.79	10.09	–4.63	12.03	843.48	33.49
E1201	318	–13.92	8.98	–2.25	10.06	1241.52	28.73
E2028	289	–0.84	6.66	–0.82	5.41	2060.94	7.87
F365	74	–19.35	12.85	–4.26	15.31	380.06	15.09
F755	412	–12.93	11.70	–4.42	10.64	780.99	21.88
F1172	412	–7.89	7.54	–2.46	6.83	1197.67	18.73
F1982	294	–1.45	6.62	–0.26	5.95	2014.03	6.74

Time series at B100, B200, B300, B400, C100, C200, C300 are from acoustic Doppler current profilers deployed at about 400 m depth on moorings B and C. Time series B440 is from an FSI current meter. All other time series are from Aanderaa current meters.

Velocities are put through a Gaussian low-pass filter with half-width of 24 hours and subsampled to daily values. The east and north velocities are then rotated by 40° to match the orientation of the local isobaths so that vd is approximately the alongshore velocity (40°T) and uc is the offshore velocity (130°T). Pressures are also given to indicate the depth of each instrument.

mooring D.

To define the offshore edge of the mean poleward flowing Agulhas Current, we laterally extrapolate the mean velocities on moorings E and F at 400, 800 and 1200 m depths (after vertically interpolating the mean velocities to the same depth on each mooring) to determine the offshore position of the zero velocity isotach. The estimated offshore edge of the time-averaged Agulhas Current is at 205, 198 or 207 km from the coast at 400, 800 or 1200 m depth, respectively. Hence, the average offshore position of the zero velocity isotach is 203 km from the coast, corresponding to a distance beyond mooring F equal to the separation between moorings E and F.

To define the depth to which the mean poleward flowing Agulhas Current penetrates, we interpolate or extrapolate the mean alongshore velocities in the vertical on each mooring to estimate the depth of the zero velocity isotach. At mooring B the zero mean velocity is estimated to be at 909 m by extrapolation while at mooring C the zero mean velocity is interpolated to be at 1210 m depth. The shallowness of the zero velocity surface at B and C reflects the presence of the Agulhas Undercurrent flowing equatorward along the continental slope. At each of the moorings D, E and F the zero velocity surface is estimated to be at 2298, 2135 and 2220 m depth, respectively. Thus, the average depth to which the poleward flowing Agulhas Current penetrates in the offshore region beyond 60 km from the coast is 2218 m or about 200 m below the deepest current meter locations.

These estimates of the offshore position and depth of the zero velocity isotach suggest that the moored current meter array provides a reasonable sampling of the main features of the Agulhas Current so that the structure and transport of the time-averaged Agulhas Current can be determined with some certainty. After discussing the temporal, vertical and lateral variability in the measured currents, we then portray the overall mean structure and estimate the mean transports within the Agulhas Current system as well as describe the temporal variability in the structure and transport.

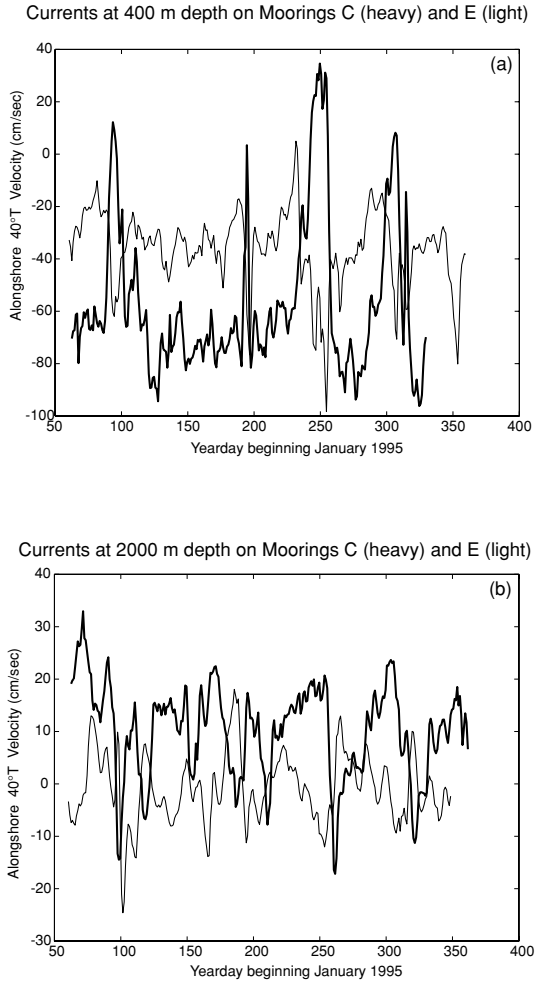

Fig. 3. Time series of alongshore (40°T) velocity on moorings C and E for a) records in the thermocline at about 400 m depth; and b) for records in the deep water at about 2000 m depth.

3. Scales of Variability within the Agulhas Current

The time series of alongshore velocity at 400 m nominal depth on moorings C and E demonstrate the character of the dominant variability in the thermocline Agulhas Current (Fig. 3(a)). For most of the record, the velocity close to the continental slope at C is strong and poleward (negative), but there are periodic episodes when the velocity close to the coast at C decreases sharply and even reverses on four occasions. The velocity at E is generally poleward but smaller in magnitude than that at C. Notably, when the poleward velocity at C decreases, the velocity at E increases sharply. In fact, the 400 m velocity records on moorings C and E are anti-correlated with a correlation coefficient of –0.47 which is significantly different from zero at 95% confidence level. These thermocline velocity time series indicate that the core of the Agulhas Current is usually quite close to the coast but that it does meander offshore occasionally. These offshore meanders of the Agulhas Current in the region southeast of Durban are sometimes called Natal Pulses.

The time series of alongshore velocity at 2000 m nominal depth on moorings C and E illustrate the differing character of the deep flows (Fig. 3(b)). The alongshore velocity at 2000 m depth on C is generally positive or northeastward, reflecting the presence of the Agulhas Undercurrent flowing equatorward along the continental slope, and it exhibits energetic variations. The comparable velocity at 2000 m depth on E oscillates about a small mean velocity with about half the variance of that at C.

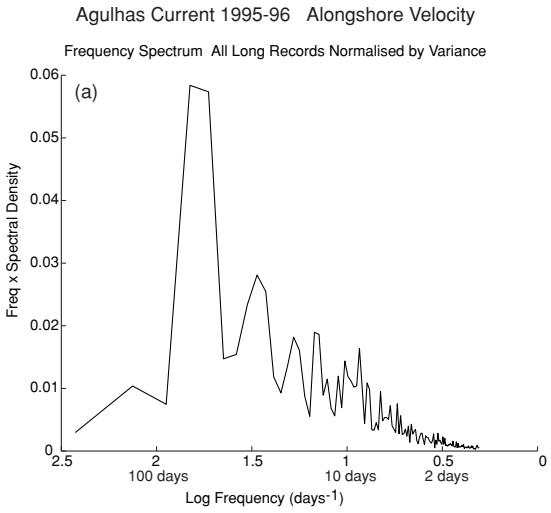

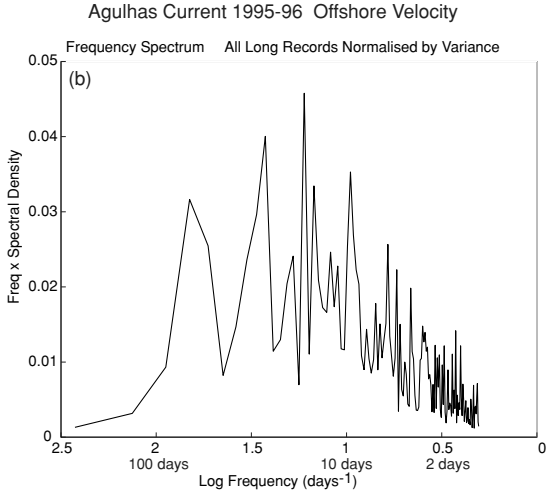

Fig. 4. Spectra for a) alongshore velocity and b) offshore velocity. Individual spectra for alongshore and offshore velocity for each of 15 records longer than 267 days are normalised and averaged to create a single composite spectrum which is then plotted in variance preserving form.

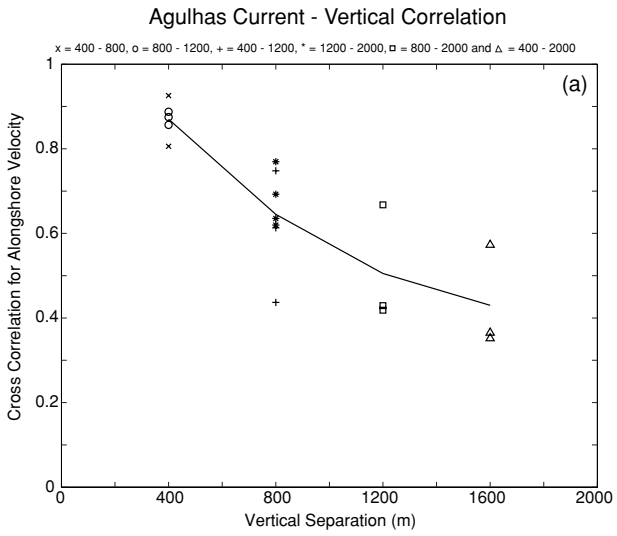

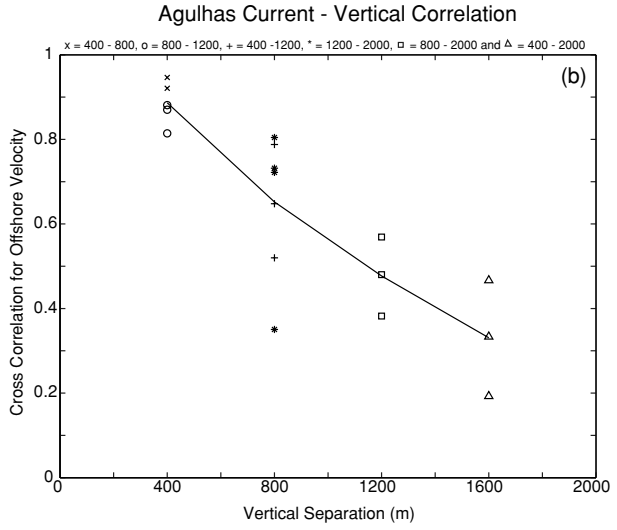

Fig. 5. Vertical correlation functions for a) alongshore velocity and b) offshore velocity. Cross-correlations for each mooring at zero time lag are estimated for each pair of records longer than 267 days and are plotted versus vertical separation.

The alongshore velocity fluctuations at 2000 m depth on moorings C and E exhibit anti-correlation with a correlation coefficient of –0.25 which is not significantly different from zero at 95% confidence level. In fact, the fluctuations in the Undercurrent at 2000 m depth on C are significantly correlated only with the fluctuations at 1200 m depth on C, which is effectively the only other instrument measuring equatorward velocities associated with the Undercurrent. Thus, the Undercurrent appears to be relatively independent of the Agulhas Current as measured by the rest of the moored current meters.

To define the temporal variability in the currents, we first calculated composite spectra for alongshore velocity and offshore velocity by averaging the spectra for 15 time series that had at least 267 daily averaged values of current. Each velocity time series was normalised to unit variance so all records are treated equally for the composite spectra. The spectrum for alongshore velocity (Fig. 4(a)) exhibits most of the variance at periods longer than 30 days. The largest peak is at periods of 53 to 67 days, indicating the 4 to 5 Natal Pulse events seen in the thermocline time series (Fig. 3(a)). The spectrum for off-

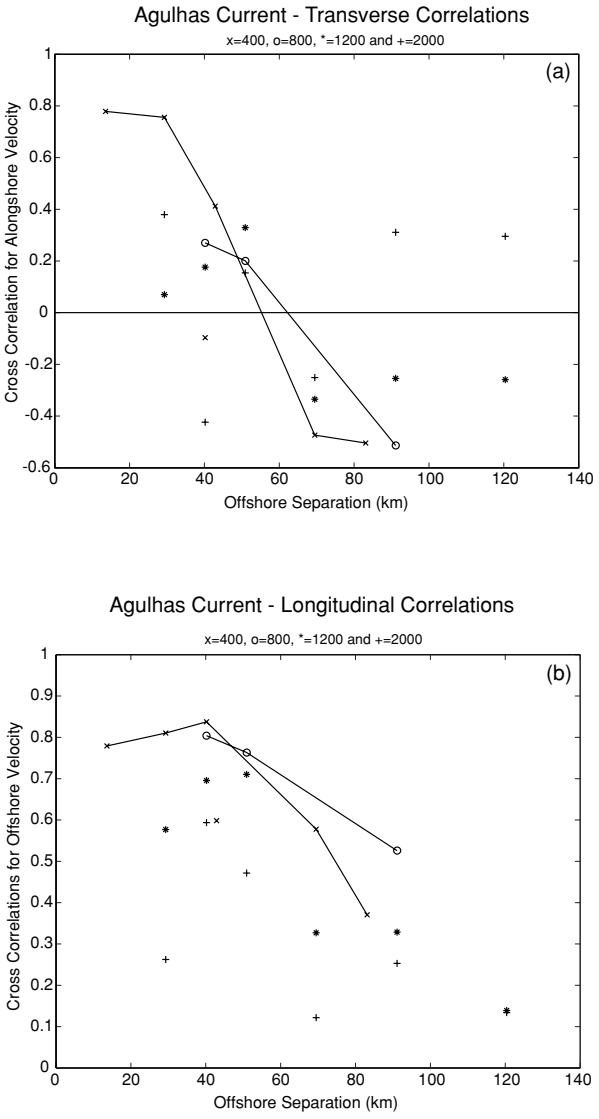

Fig. 6. Transverse (a) and longitudinal (b) correlation functions. Cross-correlations between alongshore velocity at zero time lag are estimated for each pair of records at the same depth and are plotted versus offshore separation for the transverse correlation; cross correlations between offshore velocity are similarly estimated and plotted for the longitudinal correlation.

shore velocity (Fig. 4(b)) exhibits relatively more energy at higher frequencies with a lesser peak at 67 day period and with several peaks between 27 and 8 day periods. To define an overall time scale, square integral time periods are estimated by summing the squares of the autocorrelation function for each instrument out to a time lag of 40 days. The average integral time scale for alongshore velocity is 10.2 days while the average for offshore velocity is 5.4 days. These integral time scales are used to determine significance levels for the correlation coefficients between the various records.

To establish the vertical scale of the fluctuations, correlations between alongshore and offshore velocity time series on the same mooring are estimated and plotted against vertical separation (Fig. 5). Correlation coefficients are very high (about 0.9) for vertical separations of 400 m and they decrease slowly to about 0.3 to 0.4 for the largest separations of 1600 m. For alongshore velocity, only the correlation coefficients between the 400 and 2000 m records on moorings C and E are below the 95% significance level. For onshore velocity only the correlation coefficient between the 400 and 2000 m records on mooring C is not significant. Thus, there is good vertical correlation among alongshore and onshore velocity fluctuations for all current meter records except at mooring C when one record is deep in the Undercurrent and the other is in the thermocline Agulhas Current.

One determination of the lateral scale of the Agulhas Current can be made from the transverse correlation function by estimating the correlations between alongshore velocities at the same depth as a function of the offshore separation between the records. Most of these correlations are not statistically significant and there is more scatter in the correlations, particularly at 1200 and 2000 m depths (Fig. 6(a)). The correlations at 400 and 800 m depths (which are connected by lines in Fig. 6), suggest that the zero crossing in the transverse correlation function for the thermocline Agulhas Current is about 60 km, which we take as the lateral scale of the fluctuations in the Agulhas Current.

The longitudinal correlation function defined by estimating the correlations between onshore velocities at the same depth as a function of the offshore separation (Fig. 6(b)) exhibits a much longer lateral scale than the transverse correlation function, as expected. All correlations involving onshore velocity are positive and nearly all are statistically different from zero. Thus, we expect that fluctuations in the onshore velocity will be coherent throughout the Agulhas Current system.

4. Construction of Velocity Sections across the Agulhas Current

To view the structure of the Agulhas Current and to make estimates of transport, the available measurements must be interpolated between the current meter locations and extrapolated up to the surface and down to depth. The goal is to produce reasonable currents from the moored instruments for as long a time as possible for the entire section from the surface down to 2400 m depth and from the coast offshore to 203 km in order to estimate the variability in structure and transport of the Agulhas Current. Naturally we will estimate time-averaged transport and structure, but the emphasis is on a re-

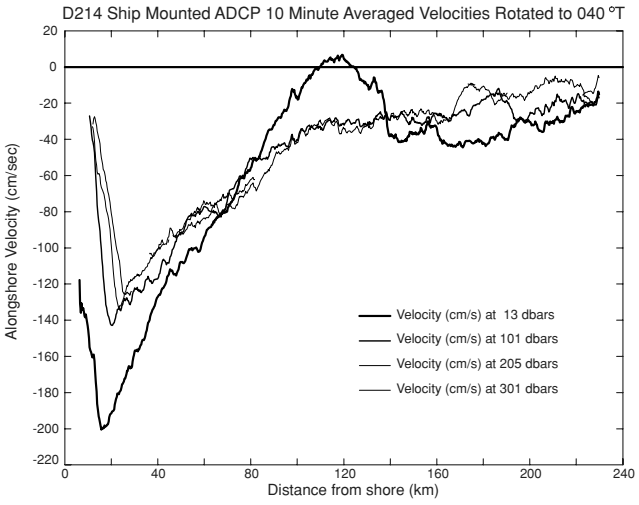

Fig. 7. Lateral structure of the alongshore velocity in the upper water observed with an underway ADCP during the mooring deployment cruise. Note the nearly linear trend toward zero at the coast in the alongshore velocity inshore from the location of strongest velocity.

alistic representation of the variability.

The first task is to fill the gaps in the short records at 800 m depth on mooring C and at 400 m on mooring F. Because of the strong vertical correlations in alongshore velocity observed in the time series measurements (Fig. 5), we fill gaps by using neighbouring records on each mooring for the period of complete data to establish by linear regression the best prediction of the alongshore velocity and then use that regression to predict the alongshore velocity during the gap. The regressions indicate that the alongshore velocities can be predicted with an rms error of 6.5 cm s^{-1} at C800 and 4.2 cm s^{-1} at F400.

Between the current meters, linear interpolation of the measured currents and their depths on a daily basis is first done vertically over each mooring to create time series at 20 m depth intervals. Horizontally, linear interpolation onto a 0.5 km lateral grid is then used at each 20 m depth interval between the moorings.

Extrapolation requires a more subjective procedure. We have based the extrapolation procedures both on the available measurements and on synoptic CTD and LADCP sections in the region (Toole and Warren, 1993; Beal and Bryden, 1999). The time series current measurements are strongly correlated in the vertical on each mooring (Fig. 5), while the lateral correlation decreases with increasing offshore separation such that the zero-crossing for the transverse correlation is at about 60 km separation. For this reason we prefer to extrapolate vertically whenever possible. Our decision was that it was reasonable to linearly extrapolate the velocities measured at 1200 and 2000 m depths only down as far as 2400 m and that is the reason for the depth limitation of the velocity section. Based on an examination of the LADCP and geostrophic velocity profiles and on the moored ADCP measurements up to the surface on moorings B and C, we concluded that the velocity profile is essentially linear above 800 m depth. Thus, extrapolation of alongshore velocity above the uppermost current meter at 400 m depth is done linearly using the 400 m and 800 m measured velocities on each mooring. For mooring B, the ADCP effectively includes a full-length record of the velocities up to 56 m depth, so only extrapolation up to the surface is required using the time series velocities at 112 and 56 m depths. For mooring C, the ADCP record stops after 45 days so extrapolation up to the surface for the remainder of the deployment is based on the 400 m and 800 m current meters. For the coincident records on mooring C, ADCP velocities at 56, 152, 256 m depths are fitted to the velocities at 400 and 800 m depth and the same fit is then applied after the ADCP record ceases in order to predict the velocities at 56, 152 and 256 m depths on mooring C. The resulting velocities are then linearly interpolated and extrapolated to provide velocities at 20 m depth intervals up to the surface.

The trickiest vertical extrapolation is the extrapolation at mooring B where the ADCP provides measurements only from 56 m to 424 m depth. Based on 1995 LADCP profiles around mooring B and 1987 and 1995 geostrophic velocity profiles from stations bracketing the position of mooring B, there appears to be a constant vertical shear in this region through the thermocline down to 940 m depth and then there is effectively no shear from 940 m to the bottom. From an empirical orthogonal function (eof) analysis of the ADCP profiles, the vertical structure through the thermocline is a combination of a constant shear (12.63 cm s^{-1} per 100 m) in mean alongshore velocity with perturbations that exhibit a weakly baroclinic structure. Extrapolation of the mean ADCP profile yields a mean alongshore current at 940 m depth of 7.21 cm s^{-1} and extrapolation of the first mode (98% of the variance) eof profile results in a perturbation amplitude at 940 m depth of 0.116 times the perturbation amplitude at 424 m depth. Thus, the predicted current at 940 m depth on mooring B has a mean northeastward direction and its variability is a scaled version of the variability measured at 424 m depth. The velocity down to 20 m above the bottom is taken to be constant, with the same value as the velocity at 940 m depth. The entire mooring B profile is then linearly interpolated to 20 m depth intervals using these predicted velocities at 940 m and 1480 m depths. As a result, the velocity below 880 m depth (the level of 0 mean velocity) at mooring B is typically northeastward, in agreement with the LADCP profiles of the Undercurrent at this location. This vertical

extrapolation effectively assumes that the baroclinic structure of the Agulhas Current remains the same throughout the mooring time series. There is evidence that the baroclinic structure does stay reasonably constant in that the geostrophic transport estimates reported by Donohue *et al*. (2000) for the 1987 and two 1995 hydrographic sections using the same reference levels were 85, 82 and 86 Sv, i.e., the same within ±2 Sv or 3%.

Extrapolation to the coast is based on the horizontal structure observed during a transect of the Agulhas Current using shipboard ADCP measurements to profile the upper waters (Fig. 7). At each depth, the alongshore velocity appears to decrease linearly from the position of the current maximum towards zero at the isobath on the continental slope. The location of mooring B at 18.8 km from the beach appears to lie shoreward of the position of maximum current at all depths. Hence, the velocity at each isobath is taken to be zero and the velocity at each depth in the wedge between mooring B and the continental slope is linearly interpolated between the value at mooring B and zero on the slope.

Extrapolation offshore from mooring F is done linearly at each depth from the velocity difference between moorings E and F. Because the offshore edge of the Agulhas Current determined from the record-length average velocities above was found to be at 203 km from the coast, the extrapolation beyond mooring F was taken out to 203 km, thus extending the section coverage beyond mooring F by the amount of the lateral separation between moorings E and F.

Using this same procedure on the record-length time-averaged currents measured on each mooring, Bryden and Beal (2001) estimated the structure of the time-averaged Agulhas Current (their figure 3) and its transport to be 70.3 Sv.

5. Variability in Structure and Transport

From the combination of first vertical then horizontal interpolation and extrapolation, daily sections of the structure and transport of the Agulhas Current from the surface to 2400 m depth and from the coast out to 203 km offshore are constructed for 267 days from 5 March to 27 November 1995. The start date is determined by the date when the last mooring was deployed and the end date is determined when both the 400 and 800 m current records on mooring C ceased, resulting in loss of confidence in structure and transport, particularly at the core of the Current around mooring C. Viewing the sequence of sections in a "movie" (the movie can be viewed at www.soc.soton.ac.uk/JRD/HYDRO/lmd/movie.html), we count 211 days when the core of maximum velocity is close to the coast at moorings B and C, 21 days when the core is at 62 km from the coast at mooring D, 30 days when the core is at mooring E 102 km from the coast,

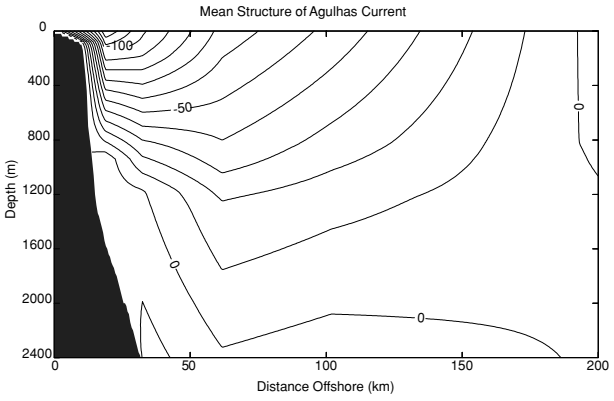

Fig. 8. Mean structure of the Agulhas Current from the 267-day averaged currents over the period from March to November of most complete instrument coverage.

and only 5 days when the core appears to be located 150 km from the coast at mooring F. Because of the extrapolation procedure used offshore of mooring F, the current increases offshore on the days when the maximum current occurs at mooring F, so the offshore currents may then not be realistic on these 5 days. Overall, the array appears to resolve the Agulhas Current almost all the time.

Transport of the Agulhas Current is estimated for each day by integrating the velocity from the coast out to 203 km and from 2400 m depth up to the surface. The integration is done by a trapezoidal procedure in which the velocity profile at each mooring (B, C, D, E, F) is assumed to be representative of the region halfway to its neighbouring moorings; in which the mooring B profile is also representative of the onshore region half the distance to the continental slope; and in which the mooring F profile is also representative of the offshore region beyond mooring F equal to 25.4 km, or half the separation between moorings E and F. This procedure yields the same transport as summing up the velocities over the 20 m depth by 0.5 km wide grid because of the linear gridding technique. Negative and positive velocities over each 20 m interval are summed separately and finally the net positive and net negative values are added to determine a single transport for each day. The transport of the Undercurrent is estimated separately by summing the velocity contributions below 900 m depth on B, below 1180 m depth on C and below the zero isotach on moorings D, E, F. Note that with such a definition the Undercurrent transport can be negative if the deep flow in the continental slope region near B and C is southward.

The time-averaged section for the 267-day period of reliable measurements from 5 March to 25 November 1995 shows an Agulhas Current closely attached to the continental slope (Fig. 8). As is characteristic of warm-

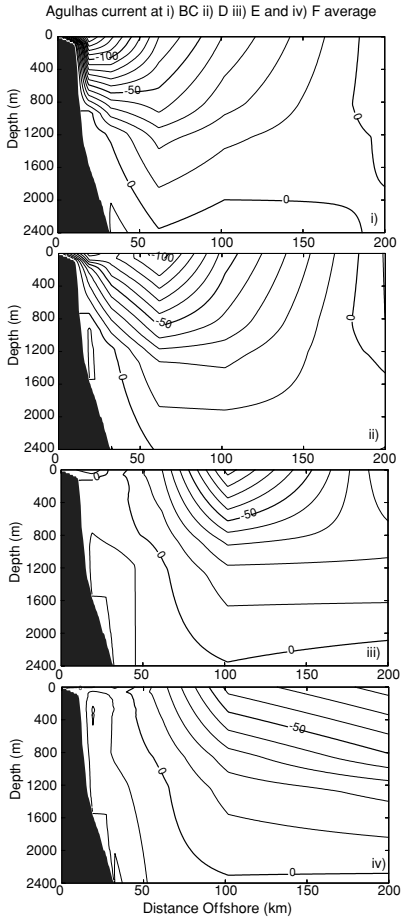

Fig. 9. Structure of the Agulhas Current when the strongest measured current at 400 m depth is located a) at mooring B or C, within 31 km of the coast; b) at mooring D, 62 km from the coast; c) at mooring E, 102 km from the coast; and d) at mooring F, 150 km from the coast.

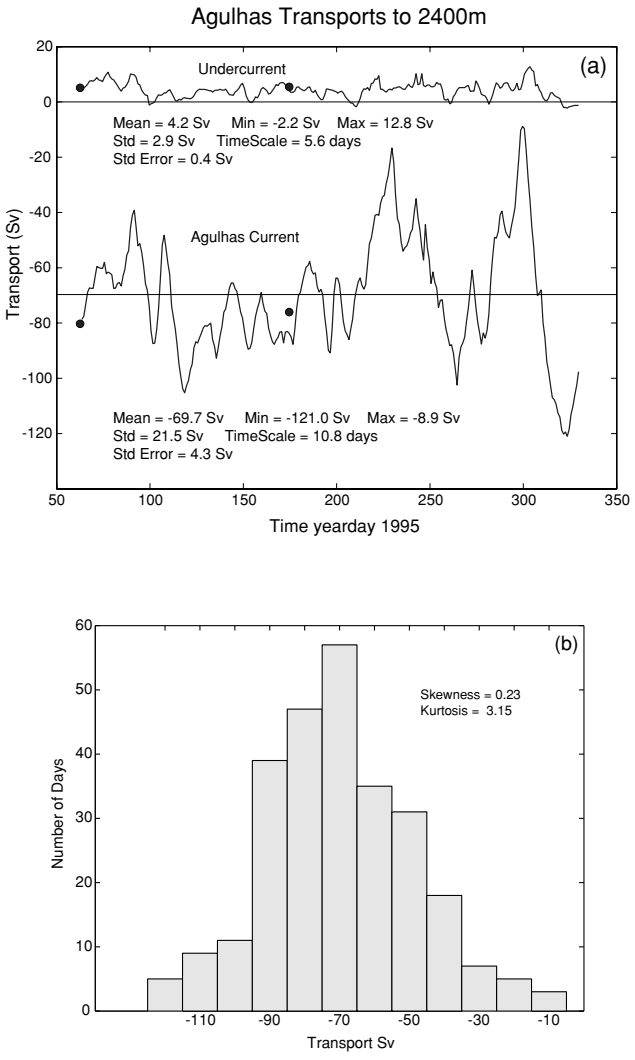

Fig. 10. (a) Time series of Agulhas Current transport and Undercurrent transport. The Agulhas Current transport on each day is estimated as the transport from the surface down to 2400 m depth and from the coast out to 203 km offshore. The Undercurrent transport is estimated as the sum of the transport below 900 m depth on mooring B plus the transport below 1180 m depth on mooring C plus the transports below the zero velocity isotach on moorings D, E and F. Darkened circles at yearday 53 and 115 denote transport estimates made from synoptic LADCP sections on board *RRS Discovery* in March 1995 and *R/V Knorr* in June 1995. (b) Histogram of daily transport values.

core western boundary currents, the position of the strongest velocity at each depth moves offshore at increasing depth: above 300 m, velocity is strongest at mooring B while the strongest velocity below 700 m is at mooring D. Far offshore, the average extrapolated velocity effectively reaches zero at a distance of 190 km from the coast. The surface of zero velocity slopes upward from 2300 m depth at an offshore distance of 60 km to intersect the continental slope at 900 m depth. Offshore of mooring D, the surface of zero velocity appears reasonably flat with no suggestion of the V-shaped reference level found during the synoptic survey by Beal and Bryden (1997). Below the zero velocity isotach, the time averaged Undercurrent hugs the continental slope. The average total transport over the entire region from the surface to 2400 m depth and from the coast to 203 km offshore is –69.7 Sv. The average transport of the Undercurrent is 4.2 Sv equatorward.

To examine the changes in structure of the Agulhas Current in its different stages, average velocity sections are constructed over the days when the maximum velocity is at mooring B or C, at mooring D, at mooring E and at mooring F (Fig. 9). Because the core of the current spends 79% of time at B and C, the structure when the maximum velocity is at B or C is similar to the time-

Table 2. Transport estimates for the Agulhas Current system.

	Agulhas Current (Sv)	Undercurrent (Sv)	Net poleward (Sv)	Net equatorward (Sv)
Transport over 267-days of best instrument coverage	−69.7	4.2	−76.2	6.5
Transport from record-length average velocities	−67.7	3.4	−70.5	2.8
Transport when maximum current is at				
18.8 km - Mooring B (126 days)	−65.6	3.9	−71.5	5.9
32.4 km - Mooring C (85 days)	−78.0	4.0	−83.3	5.3
61.7 km - Mooring D (21 days)	−86.9	2.7	−91.7	4.8
101.9 km - Mooring E (30 days)	−54.6	6.7	−67.0	12.4
152.8 km - Mooring F (5 days)	−51.8	7.3	−65.7	13.9
Synoptic transport				
5–9 March	−73.1	6.0	−79.5	6.4
22–25 June	−83.8	4.6	−88.6	4.8

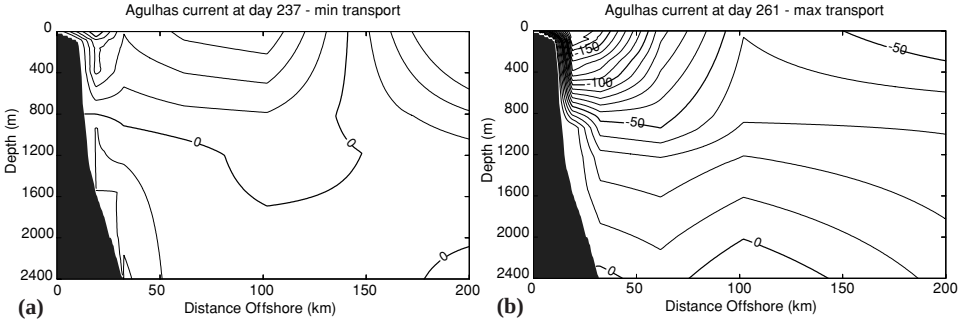

Fig. 11. Structure of the Agulhas Current on the day when the transport is a minimum (a) and a maximum (b). Minimum transport is observed on 27 October and maximum transport on 20 November 1995.

averaged section. When the strongest velocity is at D, the Agulhas Current appears to penetrate deeper with strong poleward velocities at 2000 m depth and indeed the total transport is largest when the Agulhas Current is centred at mooring D, 62 km from the coast (Table 2). The Undercurrent also appears to become a little stronger as the Agulhas Current moves offshore, but some of the increase in Undercurrent transport when the Current is centred offshore at E or F is due to the presence of northeastward velocities throughout the water column close to the coast, indicative of a warm-core eddy close to the continental slope.

The time series of Agulhas Current transport (Fig. 10(a)) indicates that the integrated transport from the surface to 2400 m, from the coast to 203 km varies between –121.0 and –8.9 Sv over the 267-day period with a standard deviation of 21.5 Sv. A histogram of daily transport values suggests that they are normally distributed with half the values between 55 and 85 Sv. From the square-integral time scale of the transport time series of 10.8 days, we estimate the standard error in this time-averaged transport to as 4.3 Sv due to the temporal fluctuations. Thus, the total transport is always poleward and we do not observe any cessation or absence of the Agulhas Current. The average poleward transport for this 267-day period estimated by summing only negative velocities each day is –76.2 Sv with a range of –122.9 to –20.5 Sv and the average equatorward transport, summing only positive velocities on each day, is 6.5 Sv with a range of 26.5 to 0.2 Sv. Even on the day of minimum total transport (27 October 1995), there appears to be a wide, shallow region of weak poleward velocities yielding a net poleward transport of –20.9 Sv but the deeper waters flowing equatorward reduce the overall transport to –8.9 Sv (Fig. 11(a)). On the day of maximum transport (20 November), the Agulhas Current close to the coast appears to be supplemented by poleward flow in an offshore eddy so that the poleward transport for the complete section is –121.9 Sv with a very small equatorward transport of 0.9 Sv (Fig. 11(b)).

These sections demonstrate how difficult it is to define the instantaneous transport of the Agulhas Current.

Should one include contributions from nearshore or offshore eddies? Should one separate out the Undercurrent? Should one average only poleward velocities? We prefer here to define the Agulhas Current transport as the total transport over a fixed region and thus we emphasise the average total transport of –69.7 Sv over the region covered by the moored array from the surface to 2400 m depth and from the coast out to 203 km. The offshore limit at 203 km is useful in that it defines the position where the average currents are zero or close to zero. With the spatially varying zero velocity surface and the presence of the Undercurrent, the depth limit for transport is somewhat more difficult to define, so we use the practical limit of 2400 m depth based on the current meters.

While the transport of the Agulhas Current estimated from a current meter array suffers from uncertainties in interpolation/extrapolation techniques, we can compare spatially resolved synoptic surveys of the Agulhas Current with the time series of transports from the array to assess whether there is a systematic offset between the synoptic transport estimates and the transports based on the array. We have recalculated the transports from the CTD/LADCP section (Beal and Bryden, 1999) during the deployment cruise to agree with the depth and offshore scales used for the current meter analyses. The resulting transport for the Agulhas Current is –80.3 Sv at a median day of 3 March compared with the array transport on 5 March (the first full day for the array) of –78.7 Sv. For the Undercurrent the LADCP transport is 5.1 Sv while the array transport is 5.2 Sv. For the synoptic CTD/LADCP section during 22–25 June 1995, Donohue *et al.* (2000) reported an Agulhas Current transport of –76 Sv and an Undercurrent transport of 5.4 Sv using definitions that closely coincide with the definitions for the array estimates. From the array measurements, the Agulhas Current transport average for 22–25 June is –83.8 Sv and the Undercurrent transport is 4.7 Sv. Thus, the synoptic section transports are in reasonable agreement with the transports from the array for the same period. Most importantly, the transports from the moored array are reasonably unbiased in reproducing the synoptic section transports which include finer spatial sampling both vertically and horizontally. We conclude that the time-averaged transport over 267 days from the moored array of –69.7 Sv ± 4.3 Sv represents a realistic estimate of the long-term average transport of the Agulhas Current at 31°S.

6. Natal Pulses

The most striking variability in the structure of the Agulhas Current is the occasional offshore meandering of the Current with associated cyclonic circulation in the nearshore region, which is called a Natal Pulse (Grïndlingh, 1979). Three to five Pulses are observed each year to propagate southwestward along the South African coast (Lutjeharms *et al.*, 2001). Their origin is variously ascribed to perturbations in the Natal bight north of Durban (de Ruijter *et al.*, 1999; van der Vaart and de Ruijter, 2001), to eddies shed off the tip of Madagascar, or even to westward propagating anomalies in the subtropical South Indian Ocean (Schouten *et al.*, 2002). When these Pulses arrive in the Agulhas retroflection region, they often appear to trigger the formation of warm Agulhas rings that move into and across the South Atlantic region (van Leeuwen *et al.*, 2000).

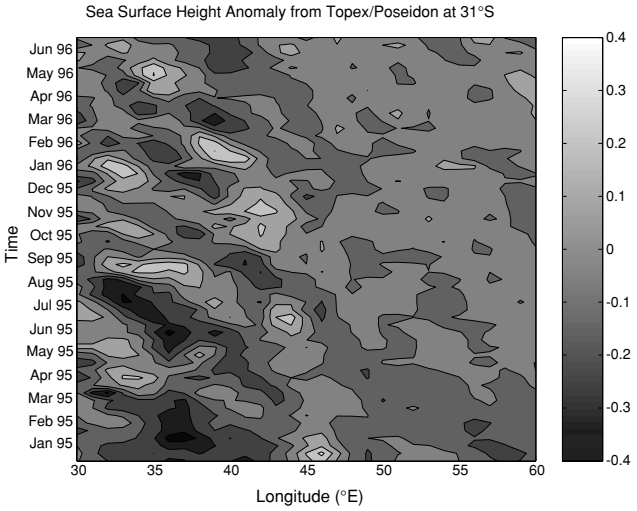

Fig. 12. Contour plot of sea surface height anomalies versus longitude and time at 31°S. Sea surface height is from the Topex-Poseidon satellite and the anomalies are with respect to three-year mean (1993–1995). In addition the average anomaly between 45°E and 110°E at each time is removed in an effort to remove much of the seasonal cycle in sea surface height. Note the low sea surface height anomalies at the western boundary in early April, September, November, December 1995 and March 1996 that correspond to Natal Pulse events as observed by the current meter array.

With the moored array we observe 5 Natal Pulse events over the period March 1995 to April 1996. Each event is primarily marked by anomalously cold waters and northward velocities throughout the water column near the continental slope. In offshore-time Hovmoller diagrams for alongshore velocity in the thermocline, northward velocity anomalies arrive simultaneously at all moorings so there is no signature of onshore-offshore propagation. Similarly, the cold temperature anomalies arrive simultaneously at all moorings, but they appear to arrive slightly later than the northward velocities. Examining the variability in sea surface height from Topex/Poseidon altimetric measurements, we believe we can see each Pulse as a low sea surface height feature near the

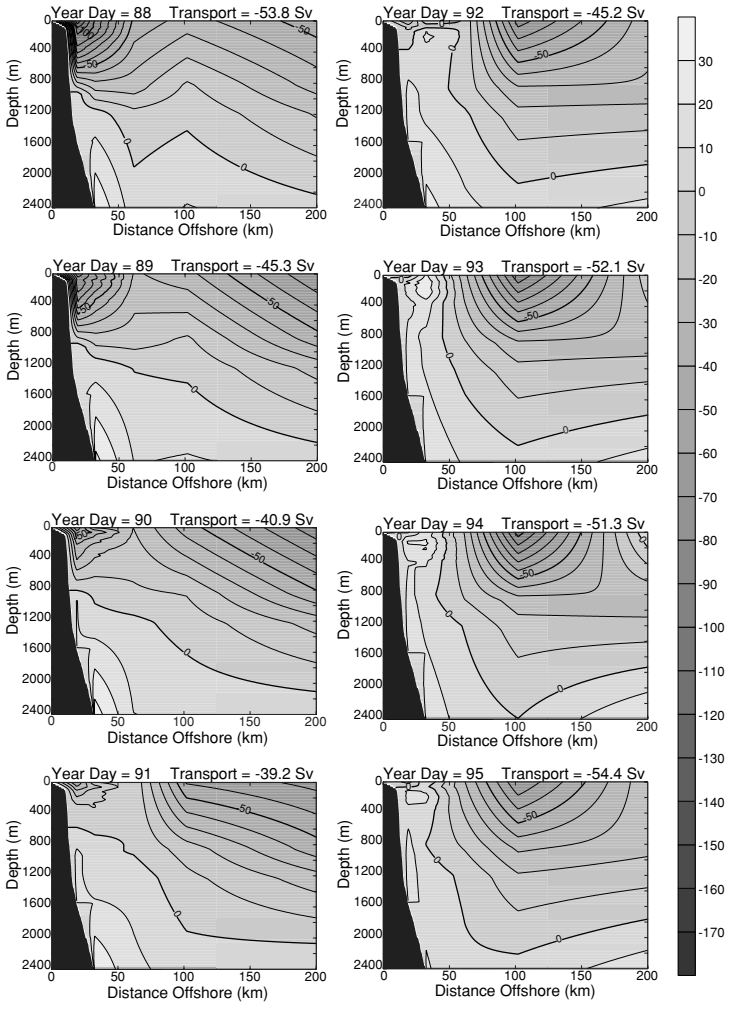

Fig. 13. Time sequence of daily averaged velocity sections during the passage of a Natal Pulse. The velocity sections are contour plots of alongshore velocity (40°T) versus depth and offshore distance determined from the current meter array measurements. Yearday 88 is 29 March 1995, yearday 95 is 5 April, and net alongshore transport is indicated for each day.

coast: in April, September, November and December 1995 and March 1996 (Fig. 12). Surprising to us is that these Pulses are not the major contributors to transport variability; that is, they do not represent maxima or minima in transport.

For the three events that are well sampled by the array measurements in April, September and November, there appears to be a consistent pattern in the arrival of the Pulses, which we illustrate in Fig. 13. First, the overall Agulhas Current weakens so that its southeastward transport becomes small and moves offshore (yeardays 88 to 91). In this weakened state, the northeastward flow of the Agulhas Undercurrent appears to penetrate upward and within a few days the Undercurrent surfaces and northward flow exists throughout the water column (yeardays 92 to 95 in Fig. 13). At the same time the strength of the Agulhas Current increases so there is a vigorous cyclonic circulation over the array. The northward flow nearshore brings with it colder temperatures so the minimum temperature occurs toward the end of the barotropic northward flow near the continental slope, for this event at yearday 95 or 96. For each of the events, the timetable is similar: first a weakened Agulhas Current followed by an apparent surfacing of the Agulhas Undercurrent with nearly barotropic northward flow over the continental slope, and finally by the appearance of very cold waters. At the time of strongest cyclonic circulation and coldest temperature, the overall southward transport of the Agulhas Current measured by the array is 54 Sv; not an anomalously low transport since it is within one standard deviation of its mean value. As noted by van der Vaart and de Ruijter (2001), there is also an associated pattern in onshore-offshore velocity where the velocity is first offshore as the Agulhas Current moves off-

Table 3. Comparison of measured western boundary current transports with Sverdrup transports.

	Latitude	Time averaged transport (Sv)	Sverdrup transport (Sv)
Agulhas Current	31°S	69.7	38.9
Brazil Current	28°S	16.2	21.2
East Australian Current	30°S	22.1	39.1
Gulf Stream	27°N	29.9	22.1
Kuroshio	24°N	21.5	32.5

Time-averaged western boundary transport for the Agulhas Current is described in this work; for the Brazil Current is reported by Muller *et al.* (1998); for the East Australian Current by Mata *et al.* (2000); for the Gulf Stream by Leaman *et al.* (1989); for the Kuroshio by Johns *et al.* (2001).

Sverdrup transport is estimated from zonally averaged wind stress curl in each basin from the SOC climatology (Josey *et al.*, 2002).

shore and then onshore as the Undercurrent surfaces so the current vectors appear to rotate counterclockwise with time. Our estimates of vertical velocity, based on the local time changes of temperature and on the horizontal advection of temperature from the vertical spiralling of the horizontal current (Bryden, 1976), indicate upwelling of 50 m to 100 m per day during the 3 to 5 days of northward velocity near the continental slope, in agreement with the vertical velocities measured by isopycnal floats (Lutjeharms *et al.*, 2001).

It should be emphasised that with these array measurements we are looking at the propagation of a Natal Pulse along the South African continental slope and not the actual formation of the Pulse. For each event that is well sampled by the array, a Natal Pulse is characterised by strong barotropic northward velocities and very cold waters near the continental slope, by large upwelling velocities, by low sea surface height near the coast in satellite altimetric time series, and by weak transport in the early stages of the Pulse but near-normal overall southward transport at the time of minimum temperature and strongest cyclonic circulation.

7. Discussion

The transport of the Agulhas Current at 31°S of 70 Sv is the largest of all the Southern Hemisphere western boundary currents measured during WOCE. The Agulhas is larger than the East Australian Current, the time-averaged transport of which was estimated at 30°S as 22.1 Sv by Mata *et al.* (2000) and larger than the Brazil Current, the time-averaged transport of which was estimated at 28°S as 16.2 Sv by Muller *et al.* (1998). Indeed, the Agulhas Current is larger than the Northern Hemisphere western boundary currents at comparable latitudes: with a transport larger than the Gulf Stream transport between 27°N and 29°N of 29 to 34 Sv (Leaman *et al.*, 1989) and larger than the Kuroshio transport between 24°N and 32°N of 21 to 42 Sv (Bingham and Talley, 1991; Johns *et al.*, 2001; Imawaki *et al.*, 2001). Thus, at a latitude of about 30°, near the centre of the subtropical gyre in each ocean, the Agulhas Current is the largest western boundary current in the World Ocean.

The Agulhas Current transport is larger than that implied by the Sverdrup transport as determined from the wind stress curl over the interior ocean. From ECMWF winds used in OCCAM (Saunders *et al.*, 1999), from Hellerman and Rosenstein (1983) wind stresses and from the SOC climatology (Josey *et al.*, 2002), the Sverdrup transport at 31°S in the Indian Ocean is estimated to be between 39 and 48 Sv, about 25 Sv less than the time-averaged Agulhas Current transport. There is an argument that the Indian Ocean Sverdrup transport ought to be augmented by the transport of the Indonesian Throughflow since the Throughflow must ultimately cross the 32°S section and probably does so as part of the western boundary current. Even adding the recent estimate for the Indonesian Throughflow of about 10 Sv (Gordon *et al.*, 1999) to the Sverdrup transport, however, still indicates that the Agulhas Current transport is about 15 Sv larger than the Sverdrup + Throughflow transport.

There is quite a difference between Sverdrup transports and western boundary current transports where time series transports have been measured. From the SOC climatology, we estimate the Sverdrup transport in each basin at a latitude corresponding to where western boundary current transports have been estimated from time series measurements (Table 3). The Gulf Stream transport through the Florida Straits at 27°N is about 30% larger than the Sverdrup transport; the Kuroshio, East Australia Current and Brazil Current transports are all much smaller than the Sverdrup transport; and notably, the Agulhas Current transport is more than 50% greater than the Sverdrup transport. While it is generally thought that all these poleward flowing western boundary currents are a result of the anti-cyclonic winds over the subtropical gyres and that their transports are quantitatively related to the

Sverdrup transport in the interior of the gyre, there appears to be no consistent relationship between Sverdrup transport and western boundary current transport where time series measurements of the western boundary current transports have been made. Quantitative understanding of the size of the wind-driven ocean circulation remains rudimentary.

Acknowledgements

The current meter measurements across the Agulhas Current were supported by the Natural Environment Research Council (NERC) under the UK WOCE Community Research Programme. We thank the South African Sea Fisheries Research Institute for arranging shiptime on *R/V Algoa* to recover the moorings, including a cruise at short notice to recover the drifting mooring B. Analysis by HLB and LMD has been supported by NERC under the Core Research Project "Observing and Modelling Seasonal to Decadal Variability in the Ocean" and under Grant NER/A/S/2000/00438. Analysis by LMB has been supported by the National Science Foundation under grants OCE99-07458 and OCE-0244769. Helpful comments by two anonymous reviewers and by editor Johann Lutjeharms led to improvements to the analysis.

References

Beal, L. M. (1997): Observations of the velocity structure of the Agulhas Current. Ph.D. Thesis, Department of Oceanography, University of Southampton, 158 pp.

Beal, L. M. and H. L. Bryden (1997): Observations of an Agulhas Undercurrent. *Deep-Sea Res. I*, **44**, 1715–1724.

Beal, L. M. and H. L. Bryden (1999): The velocity and vorticity structure of the Agulhas Current at 32°S. *J. Geophys. Res.*, **104**, 5151–5176.

Bingham, F. M. and L. D. Talley (1991): Estimates of Kuroshio transport using an inverse technique. *Deep-Sea Res.*, **38** (Suppl.), S21–S43.

Bryden, H. L. (1976): Horizontal advection of temperature for low-frequency motions. *Deep-Sea Res.*, **23**, 1165–1174.

Bryden, H. L. and L. M. Beal (2001): Role of the Agulhas Current in Indian Ocean circulation and associated heat and freshwater fluxes. *Deep-Sea Res. I*, **48**, 1821–1845.

Bryden, H. L. *et al*. (1995): *RRS Discovery* cruise 214, 26 Feb–09 Mar 1995: Agulhas Current Experiment. Cruise Report 249, Institute of Oceanographic Sciences, Wormley, 85 pp.

de Ruijter, W. P. M., P. J. van Leeuwen and J. R. E. Lutjeharms (1999): Generation and evolution of Natal Pulses: Solitary meanders in the Agulhas Current. *J. Phys. Oceanogr.*, **29**, 3043–3055.

Donohue, K. A., E. Firing and L. Beal (2000): Comparison of three velocity sections of the Agulhas Current and Agulhas Undercurrent. *J. Geophys. Res.*, **105**, 28585–28593.

Gordon, A. L., R. D. Susanto and A. Ffield (1999): Throughflow within Makassar Strait. *Geophys. Res. Lett.*, **26**, 3325–3328.

Grïndlingh, M. L. (1979): Observation of a large meander in the Agulhas Current. *J. Geophys. Res.*, **84**, 3776–3778.

Grïndlingh, M. L. (1980): On the volume transport of the Agulhas Current. *Deep-Sea Res.*, **27A**, 557–563.

Grïndlingh, M. L. (1983): On the course of the Agulhas Current. *South African Geographical Journal*, **65**, 49–57.

Hellerman, S. and M. Rosenstein (1983): Normal monthly wind stress over the world ocean with error estimates. *J. Phys. Oceanogr.*, **13**, 1093–1104.

Imawaki, S., H. Uchida, H. Ichikawa, M. Fukasawa, S. Umatani and the ASUKA Group (2001): Satellite altimeter monitoring the Kuroshio transport south of Japan. *Geophys. Res. Lett.*, **28**, 17–20.

Johns, W. E., T. N. Lee, D. Zhang and R. Zantopp (2001): The Kuroshio east of Taiwan: Moored transport observations from the WOCE PCM-1 Array. *J. Phys. Oceanogr.*, **31**, 1031–1053.

Josey, S. A., E. C. Kent and P. K. Taylor (2002): Wind stress forcing of the ocean in the SOC climatology: Comparisons with the NCEP/NCAR. ECMWF, UWM/COADS and Hellerman and Rosenstein datasets. *J. Phys. Oceanogr.*, **32**, 1993–2019.

Leaman, K. D., E. Johns and T. Rossby (1989): The average distribution of volume transport and potential vorticity with temperature at three sections across the Gulf Stream. *J. Phys. Oceanogr.*, **19**, 36–51.

Lutjeharms, J. R. E., O. Boebel, P. C. F. van der Vaart, W. P. M. de Ruijter, T. Rossby and H. L. Bryden (2001): Evidence that the Natal Pulse involves the Agulhas Current to its full depth. *Geophys. Res. Lett.*, **28**(18), 3449–3452.

Mata, M. M., M. Tomczak, S. Wijffels and J. A. Church (2000): East Australian Current volume transports at 30°S: Estimates from the World Ocean Circulation Experiment hydrographic sections PR11/P6 and the PCM3 current meter array. *J. Geophys. Res.*, **105**, 28509–28526.

Muller, T. J., Y. Ikeda, N. Zangenberg and L. V. Nonato (1998): Direct measurements of western boundary currents off Brazil between 20°S and 28°S. *J. Geophys. Res.*, **103**, 5429–5437.

Saunders, P. M., A. C. Coward and B. A. de Cuevas (1999): Circulation of the Pacific Ocean seen in a global ocean model: Ocean Circulation and Climate Advance Modelling project (OCCAM). *J. Geophys. Res.*, **104**, 18281–18299.

Schouten, M. W., W. P. M. de Ruijter and P. J. van Leeuwen (2002): Upstream control of Agulhas Ring shedding. *J. Geophys. Res.*, **107**(C8), 10,1029/2001JC000804.

Toole, J. M. and M. E. Raymer (1985): Heat and fresh water budgets of the Indian Ocean-revisited. *Deep-Sea Res.*, **32**, 917–928.

Toole, J. M. and B. A. Warren (1993): A hydrographic section across the subtropical South Indian Ocean. *Deep-Sea Res. I*, **40**, 1973–2019.

van der Vaart, P. C. F. and W. P. M. de Ruijter (2001): Stability of western boundary currents with an application to pulselike behavior of the Agulhas Current. *J. Phys. Oceanogr.*, **31**, 2625–2644.

van Leeuwen, P. J., W. P. M. de Ruijter and J. R. E. Lutjeharms (2000): Natal pulses and the formation of Agulhas rings. *J. Geophys. Res.*, **105**, 6425–6436.